Journal of Applied Polymer Science

Effect of pigmentation on polyurethane/polysiloxane hybrid coatings

Tongzhai Gao,[1] Enrique Maya-Visuet,[2] Zhouying He,[1] Homero Castaneda-Lopez,[2] Irina J. Zvonkina,[1] Mark D. Soucek[1]

[1]Department of Polymer Engineering, the University of Akron, Akron Ohio 44325

[2]Department of Chemical and Biomolecular Engineering, National Center for Education and Research on Corrosion and Materials Performance (NCERCAMP), the University of Akron, Akron Ohio 44325

Correspondence to: M. D. Soucek (E-mail: msoucek@uakron.edu)

ABSTRACT: Rutile TiO_2 was formulated into polyurethane/polysiloxane hybrid coatings in order to investigate the influence of pigmentation on the inorganic phase of the hybrid coatings. Two urethanes were prepared from the isocyanurate of hexane diisocyanate (HDI), alkoxysilane modified HDI, and tetraethyl orthosilicate (TEOS) oligomers, with oligoesters derived from either cyclohexane diacids (CHDA) and 2-butyl-2-ethyl-1,3-propanediol (BEPD) or adipic acid (AA), isophthalic acid (IPA), 1,6-hexanediol (HD), and trimethylol propane (TMP). The oligoesters were spectroscopically characterized using GPC, FT-IR, and NMR. Chemical interaction between the TiO_2 and the sol–gel precursor was investigated using solid-state ^{29}Si NMR and XPS. The morphology, mechanical, viscoelastic, thermal properties of the pigmented coatings are evaluated as a function of pigmentation volume concentration (PVC). Using AFM and SEM, the pigment was observed to be well dispersed in the polymer binder. The thermal stability, the tensile modulus, and strength of the coatings were enhanced with increasing PVC, whereas the pull-off adhesion and flexibility (elongation-at-break) were reduced with increasing PVC. Finally, the pigmented coatings were evaluated by electrochemical impedance spectroscopy (EIS) and the results showed that 10 wt % of the pigment improved the corrosion resistance of the entire coating system. © 2015 Wiley Periodicals, Inc. J. Appl. Polym. Sci. **2016**, *133*, 42947.

KEYWORDS: corrosion resistance; hybrid coatings; pigmentation; sol–gel process; titanium dioxide

Received 5 August 2015; accepted 15 September 2015

DOI: 10.1002/app.42947

INTRODUCTION

The recent decades have seen an increasing interest in developing organic/inorganic hybrid materials for a plethora of applications, such as coatings,[1,2] solar cells,[3,4] sensors,[5] etc. Particularly, inorganic/organic coatings have received much attention. The term "ceramer" was coined to define a material containing both ceramic and polymeric components.[6] This type of material incorporates colloidal inorganic particles into an organic matrix via the sol–gel process yielding physical properties superior to the conventional polymers. The sol–gel process has been extensively applied in synthesizing novel inorganic/organic materials. Depending on the selection of the starting material, a variety of interactions between the inorganic and organic phase may occur. One of the initiatives of using inorganic/organic coatings is to provide corrosion protection of the metal surface.

Polyurethane coatings play a vital role in the application as a high performance topcoat for automotive and airplanes.[7] Polyurethane/polysiloxane TEOS-based self-priming coating or "unicoat" system were recently developed to replace the chromate pretreatment, primer, and topcoat system for aircraft.[8–10] In this system, polyurethane provides the general mechanical properties and polysiloxane functions as an adhesion promoter and corrosion inhibitor. A hybrid coating system was formulated using the alkoxysilane-functionalized isocyanurate and HDI isocyanurate, cycloaliphatic polyesters in combination of the TEOS oligomers. The combination of alkoxy and TEOS at the metal/organic film interface dramatically enhanced the adhesion. The polysiloxane formed by the sol–gel process had a significant effect on the corrosion inhibition.

As a complication to the academic research, coatings can be formulated with pigments (and filler), which can reach as high as 80–90% by weight or 70% by volume.[11] Arguably, titanium dioxide (TiO_2) is one of the most important pigment used in the coatings industry. Because of the high large surface-area/particle-size ratio and the incompatibility with polymeric matrix, TiO_2 particles tend to strongly aggregate as well as potentially interact with other components in the coating formulation. This raised a crucial concern that how the components interacted with each other, especially how the pigmentation affected the sol–gel process.

© 2015 Wiley Periodicals, Inc.

A great number of research has been focused on the surface modification of TiO_2 using alkoxysilanes in order to achieve proper dispersion and increase the compatibility with the polymer matrix, such as polyacrylate,[12] polycarbonate,[13] silicon elastomer,[14] polystyrene,[15] epoxide,[16] poly(methyl methacrylate),[17] unsaturated polyester,[18] nylon,[19] and polyurethane.[20–22] With respect to polyurethane/TiO_2 composite system, the surface-treated pigments had a better dispersion, smaller agglomeration, and a lower surface roughness than the untreated counterpart. No efforts were put into studying the covalent bonding between the silanes and the pigments. Polyurethane/(TiO_2-SiO_2) composite system was also investigated where both TiO_2 and SiO_2 were prepared via sol–gel process and form a covalent bond with the organic phase.[23] The covalent bonding between the alkoxysilanes and TiO_2 particles have been separately studied,[24–28] but without further investigation by incorporating into a polymer matrix. To date, no study has been found on TiO_2 pigmented polymer/inorganic hybrid system where the inorganic phase was prepared via *in situ* sol–gel process, particularly the interactions between the pigment and the sol–gel precursors.

To investigate the effect of pigmentation on the polyurethane/polysiloxane hybrid coatings, TiO_2 pigment was incorporated into the hybrid system. Polyurethane/polysiloxane hybrid coatings were formulated with different pigment volume concentration (PVC). The control samples were prepared using the same loading of titanium dioxide (10–40 wt %) while any component containing silicon was omitted including the coupling agent. The interaction between the TiO_2 nanoparticles and the siloxane moiety in the coatings was investigated by solid-state ^{29}Si NMR and X-ray photoelectron spectroscopy (XPS). The dispersion of the pigments was examined by SEM and AFM. The thermal behavior was studied by DSC and TGA and the viscoelastic properties were determined by DMTA. The impact of PVC on the mechanical properties and overall coating performance was also evaluated. The corrosion resistance of the pigmented coatings was investigated by electrochemical impedance spectroscopy (EIS).

EXPERIMENTAL

Materials

The HDI isocyanurate (abbreviated as 3HDI) was supplied by Bayer Material Science (Desmodur N-3300, unstabilized). The 1,3 and1,4-cyclohexane diacid (CHDA, 97%), 2-butyl-2-ethyl-1,3-propanediol (BEPD, 99%), adipic acid (AA, 99%), isophthalic acid (IPA, 99%), 1,6-hexanediol (HD, 97%), trimethylolpropane (TMP, 98%), dibutyltin(IV) oxide (DBTO, 98%), methyl ethyl ketone (MEK, ≥99.9%), 3-aminopropyltriethoxysilane (APTES, ≥98%), rutile titanium(IV) dioxide (TiO_2, 99.99% trace metals basis), the antifoam agent, sodium chloride (ACS reagent, ≥99.0%), and hydrochloric acid (36.5–38.0%, Bioreagent, for molecular biology) were purchased from Sigma–Aldrich and used as received. The dispersing agent, DISPERBYK-2155, was provided by BYK. TEGO Wet KL 245 was obtained from Evonik. Aluminum panels (3003 H14, 3 × 6 in^2) were acquired from Q-panel Lab Products. The glass plates were obtained from local North Hill Glass & Mirror Company.

Synthesis of Polyesters

Synthesis of CHDA-BEPD Polyester. The CHDA-BEPD polyester was prepared using a typical step polymerization technique as described in the literature.[29] The following formulation was utilized to synthesize the polyester: 1,3-CHDA (55.25 g, 0.33 mol), 1,4-CHDA (168.75 g, 0.99 mol), BEPD (329.84 g, 2.06 mol), xylene (18.15 g, 0.17 mol), DBTO (2.22 g, 0.0089 mol). A 500-mL reactor was equipped with mechanical stirrer and nitrogen purge, a Dean-Stark trap used to collect the byproduct (water). The reaction was performed under nitrogen purge and the maximum temperature at the post stage was kept at 210°C. The end of the esterification reaction was determined by the acid number when it reached a value below 10 mg KOH g^{-1} resin (according to ASTM D1639-89). The hydroxyl number was determined according to ASTM D 4274-94 to be 146.7 mg KOH g^{-1} resin, respectively. The molecular weight (M_n) was measured by gel permeation chromatography (Waters Breeze GPC, PS standard) to be 1148 (PDI: 1.25). The chemical structure was analyzed by FTIR and NMR and the assignments were listed as below:

FTIR: 3100–3650 cm^{-1} (—OH), 2931 cm^{-1} (ν_{as} CH_2), 2865 cm^{-1} (ν_{sym} CH_2), 1725 cm^{-1} (ν (C=O) ester), 1460 cm^{-1} (δ CH_2), 1380 cm^{-1} (δ CH_3), 1238 cm^{-1} (ν (C=O) + ν (O—CH_2) ester)

^1H NMR: (300 MHz, $CDCl_3$), δ 7.07 (—O<u>H</u>), 3.92, 3.98 (COOC<u>H</u>$_2$), 3.59 (—C<u>H</u>$_2$OH), 2.32 (—CH_2C<u>H</u>CH_2—, cyclohexane), 2.05 (—CHC<u>H</u>$_2$CH—, cyclohexane), 1.89 (—CHC<u>H</u>$_2$ CH_2—, cyclohexane), 1.58 (—CH_2C<u>H</u>$_2CH_2$—, cyclohexane), 1.27 (—CH_2C<u>H</u>$_2CH_2$—, BEPD), 0.92 (—C<u>H</u>$_2CH_3$), 0.85 CH_2C<u>H</u>$_3$).

^{13}C NMR: δ 175.56 (<u>C</u>=O), 69.08 (COO<u>C</u>H$_2$), 66.34 (<u>C</u>H$_2$OH), 42.63, 41.26, 39.58 (—CH_2<u>C</u>HCH_2—, cyclohexane), 29.64 (—CH_2 <u>C</u>H_2C—, BEPD), 26.06 (—<u>C</u>H$_2CH_2CH_3$, butyl), 23.48 (—CH_2 <u>C</u>H_2CH_3, butyl), 14.02 (—CH_2CH_2<u>C</u>H_3, butyl), 7.09 (—CH_2<u>C</u>H_3, ethyl).

Synthesis of AA-IPA-HD-TMP Polyester. A similar procedure was used to synthesize AA-IPA-HD-TMP polyester and the formulation was given as: AA (160 g, 1.1 mol), IPA (181.87 g, 1.1 mol), HD (258.74 g, 2.2 mol), TMP (73.44 g, 0.55 mol), xylene (45.87 g, 0.43 mol), DBTO (2.70 g, 0.011 mol). The hydroxyl number was 131.4 mg KOH g^{-1} resin and the molecular weight was 1188 (PDI: 1.29). The chemical structure was confirmed by FTIR and NMR shown as below.

FTIR: 3100–3700 cm^{-1} (—OH), 2932 cm^{-1} (ν_{as} CH_2), 2863 cm^{-1} (ν_{sym} CH_2), 1725 cm^{-1} (ν (C=O) ester), 1462 cm^{-1} (δ CH_2), 1387 cm^{-1} (δ CH_3), 1235 cm^{-1} (ν (C=O)+ ν (O-CH_2) ester)

^1H NMR: δ 8.68, 8.21, 7.53 (aromatic protons), 7.07 (—O<u>H</u>), 4.37 (COOC<u>H</u>$_2$, IPA), 4.08 (COOC<u>H</u>$_2$, AA), 3.65 (—C<u>H</u>$_2$OH), 2.31 (O=C—C<u>H</u>$_2CH_2$—), 1.82 (—OC<u>H</u>$_2$C<u>H</u>$_2CH_2$—), 1.66 (O=C —CH_2C<u>H</u>$_2$—), 1.48 (—CH_2C<u>H</u>$_2$C<u>H</u>$_2CH_2$—, AA), 0.88 (—CH_2 C<u>H</u>$_3$).

^{13}C NMR: δ 173.31 (<u>C</u>OOCH$_2$, AA), 165.73 (<u>C</u>OOCH$_2$, IPA), 133.57, 130.56, 128.79 (benzene ring), 65.17, 64.20, 62.61 (COO<u>C</u>H$_2$), 33.82 (COOCH$_2$<u>C</u>H$_2$, IPA), 28.51 (COOCH$_2$<u>C</u>H$_2$, AA), 25.64 (—CH_2<u>C</u>H$_2$<u>C</u>H$_2CH_2$—, HD), 24.33 (—CH_2<u>C</u>H$_2$<u>C</u>H$_2$ CH_2—, AA), 7.32 (—CH_2<u>C</u>H$_3$).

Table I. Formulation of Pigmented Polyurethane/Polysiloxane Hybrid Coatings

TiO_2 wt. ratio	10%	20%	30%	40%
PVC	3%	7%	11%	16%
TiO_2/g	1.00	2.00	3.00	4.00
MEK/g	5.00	5.00	5.00	5.00
Disperbyk/g	0.04	0.08	0.12	0.16
Wetting agent/g	0.02	0.04	0.06	0.08
Polyester[a]/g	4.68	4.16	3.64	3.12
3HDI/g	1.72	1.53	1.34	1.15
3HDI-APTES/g	2.15	1.91	1.67	1.43
TEOS oligomer/g	0.45	0.40	0.35	0.30
Antifoam agent/g	0.09	0.08	0.07	0.06

[a] CHDA-BEPD and AA-IPA-HD-TMP.

Monofunctionalization of Hexamethylene Diisocyanate (HDI) Isocyanurate

The HDI isocyanurate was modified by reacting HDI isocyanurate (3HDI) and 3-aminopropyltriethoxysilane (APTES) with a molar ratio 1:1.[30] The 3-APTES (6.63 g, 0.3 M, molarity) was dissolved in acetone (33.2 mL) producing a 20% 3-APTES solution. A 20% solution of HDI isocyanurate was obtained by mixing HDI isocyanurate (5.82 g, 0.3 equiv. —NCO, normality) and acetone (29.1 mL). The 3-APTES solution was added dropwise into the flask containing HDI isocyanurate solution at 25°C. After addition, the reactants were stirred for 1 h. The acetone was then removed by vacuum at ambient temperature to afford the final product.

^{1}H NMR: δ 5.44–5.79 (—NHCOOC$_2$H$_5$ and —NHCONH—), 4.08 (—COOCH$_2$CH$_3$), 3.76–3.97 [(—CO)$_2$NCH$_2$— and —Si(OCH$_2$CH$_3$)$_3$], 3.05–3.35 (—CH$_2$COO— and —CH$_2$NHCONHCH$_2$—), 1.15–1.75 [—CH$_2$(CH$_2$)$_4$CH$_2$—, —COOCH$_2$CH$_3$, and —CH$_2$CH$_2$Si(OCH$_2$CH$_3$)$_3$], 0.62 (—CH$_2$Si—).

^{13}C NMR: δ 158.62 (—NHCONH—), 156.63 (—NHCOOCH$_2$—), 148.61 [(—CO)$_2$N—],60.0 [—COOCH$_2$—], 57.88 [—Si(OCH$_2$CH$_3$)$_3$], 42.42, 40.44, 39.61, 30.03, 29.39, 27.32, 26.09, 25.91, 23.43 [— (CH$_2$)$_6$— and —NHCH$_2$CH$_2$CH$_2$Si—], 18.04 [—Si(OCH$_2$CH$_3$)$_3$], 14.42 (—COOCH$_2$CH$_3$), 7.22 (—CH$_2$Si—).

ESI-MS: base peak 840 Da.

Preparation of TEOS Oligomers

Ethanol (44.16 g, 0.96 mol) was utilized as a solvent to dissolve tetraethylorthosilicate (TEOS, 50 g, 0.24 mol) in a round-bottom flask (250 mL) and distilled water (4.32 g, 0.24 mol) was then introduced into the mixture. After the mixture became homogeneous, hydrochloric acid (36.5–38.0 wt % in water, 0.99 mL) was added dropwise while the reactants were stirred with a magnetic bar. The reaction was allowed to proceed for 48 h at ambient temperature. Finally, the solvent was removed at 50°C to afford TEOS oligomers (32.55 g, 65.1% yield based on TEOS). The products were characterized by ^{1}H and ^{29}Si NMR.

^{1}H NMR: δ 3.82–3.93 (multiplet, oligomeric species), 1.21 (—SiOCH$_2$CH$_3$)

^{29}Si NMR: δ −88.0 [Si—O—Si(OCH$_2$CH$_3$)$_2$—O—Si, cyclic trimer], −89.0 [Si—O—Si(OCH$_2$CH$_3$)$_3$, end group], −94.1 [Si—O—Si(OH)(OCH$_2$CH$_3$)—O—Si, cyclic ring], −95.3 [Si—O—Si(OCH$_2$CH$_3$)$_2$—O—Si, cyclic ring], −96.4 [Si—O—Si(OCH$_2$CH$_3$)$_2$—O—Si, linear], −101.6 [Si—O—Si(OH)(OSi) —O—Si, linear], −103.1 [Si—O—Si(OCH$_2$CH$_3$)(OSi)—O—Si, cyclic ring].

Control Samples for Solid State ^{29}Si NMR

The samples of the hybrid composition were prepared according to the formulation corresponded to the 10 wt % of titanium dioxide that was proven to demonstrate the best anticorrosion behavior. The control solid samples contained TEOS oligomer, TiO_2 and TEOS oligomer (0.5 and 0.23 g, respectively), APTES used as a coupling agent, TiO_2 and APTES (0.5 and 1.08 g, respectively) and TiO_2, APTES, and TEOS oligomer (0.5, 1.08, and 0.23 g, respectively).

Formulation and Preparation of Pigmented Polyurethane/Polysiloxane Hybrid Coatings

The formulations were made by varying the amount of TiO_2 from 10 to 40 wt % (estimated pigment volume concentration was also calculated) as shown in Table I. Table II shows the formulation of the control samples, which do not contain siloxane components. For the binder part, the molar ratio of isocyanate group to hydroxyl group was kept constant at 1.1/1.0. The weight ratio between the mono-functionalized 3HDI and the unmodified 3HDI were kept at 1.2. The coatings were prepared by a 2K system, one component containing TiO_2, dispersing agent (DISPERBYK 2155), wetting agent (TEGO WET KL245), polyester and MEK, and the other having 3HDI, 3HDI-APTES, TEOS oligomers, antifoam agent, and MEK. Both components were mixed well and then combined into a container with vigorous mixing using a stirrer for about 10 min. There was a 5-min delay after stirring and before casting to allow for degassing of the formulations Aluminum panels obtained from Q-panel were degreased with acetone; the films were cast on the aluminum panels with the thickness of 100 μm (4 mil) by a drawbar for the general coating tests and EIS measurement, and on the glass plates with the thickness of 125.0 μm (5 mil) for the solid state NMR, XPS, DMTA, tensile, thermal, SEM, AFM tests. The coatings were cured at 120°C for 30 min. The cured films were stored for 3 days under ambient atmospheric conditions before testing. The samples were designated by the polyester used and the corresponding TiO_2 content. For example, PU_CHDA_H_Ti10 is a polyurethane hybrid

Table II. Formulation of Pigmented Polyurethane Coatings (Control)

TiO_2 wt. ratio	10%	20%	30%	40%
PVC	3%	7%	11%	16%
TiO_2/g	1.00	2.00	3.00	4.00
MEK/g	5.00	5.00	5.00	5.00
Polyester[a]/g	5.65	5.02	4.40	3.77
3HDI/g	3.35	2.98	2.60	2.23
Antifoam agent/g	0.09	0.08	0.07	0.06
Dispersant/g	0.04	0.08	0.12	0.16
Wetting agent/g	0.02	0.04	0.06	0.08

[a] CHDA-BEPD and AA-IPA-HD-TMP.

coating based on CHDA-BEPD polyester containing 10 wt % TiO_2 and PU_CHDA_C_Ti10 is the control polyurethane coating based on CHDA-BEPD polyester with 10 wt % TiO_2 without any siloxane component.

Instrumentation

^{1}H, ^{13}C, and ^{29}Si NMR. ^{1}H and ^{13}C NMR spectra were obtained from a Mercury-300 spectrometer (Varian) in chloroform, and liquid ^{29}Si NMR was recorded on a Geminin-400 spectrometer (Varian) at room temperature. Solid state ^{29}Si NMR spectra were recorded on a Varian Direct-Drive 500 MHz (11.7 T) spectrometer equipped with VnmrJ 3.2A software, five broad-band rf channels, and a Varian narrow-bore, triple-resonance T3HXY NMR probe at room temperature. The samples were packed into 4 mm zirconia rotors and collected with magic-angle scanning (MAS) at a spinning speed of 15 kHz. ^{29}Si CP MAS NMR spectra were collected with a spectral width of 50 kHz, a 0.01536-s acquisition time, a 5-s relaxation delay, a 4-ms contact time, and 50 kHz TPPM ^{1}H decoupling.

Solid state ^{29}Si NMR was performed for the pigmented polyurethane-polysiloxane hybrid coating compositions and for the control samples that were prepared without a polymer binder.

X-ray Photoelectron Spectroscopy (XPS). X-ray photoelectron spectroscopy (XPS) analyses were performed in a PHI VersaProbe II Scanning XPS Microprobe. The pass energy was set to 25 and 0.1 eV for the survey and the narrow scans, respectively. The spectra were recorded with a pass energy of 25 eV in 0.1 eV steps at a pressure below 6×10^{-7} mbar. The C 1s peak was used as an internal reference with a binding energy of 284.8 eV. High-resolution XPS spectra were acquired by Gaussian/Lorentzian curve fitting after S-shape background subtraction.

Dynamic Mechanical Thermal Analysis (DMTA). The viscoelastic properties were measured on a dynamic mechanical thermal analyzer (DMTA, Q800, TA Instruments) with a frequency of 1 Hz and a heating rate of 3.0°C min^{-1} over a range of −50–150°C. The gap distance was set up at 4 mm for rectangular specimens (10 mm × 6 mm × 0.05–0.10 mm). Glass transition temperature (T_g) of the crosslinked pigmented coating films were determined from the tan δ vs. temperature plots.

Mechanical Properties. The mechanical properties of the pigmented films were performed on an Instron 5567 tester (Instron, Grove City, PA) according to ASTM D2370-2010. The films were cast on the glass plate in order to easily remove for sample preparation. The sample dimensions were 0.09–0.11 mm in thickness, 13 mm in width, and 25 mm in length. A crosshead speed of 10 mm min^{-1} was applied. All the testing was carried out at room temperature. The modulus, tensile stress, and elongation at break were recorded. The average value and the standard deviation were obtained based on the measurement of 10 replicates.

Thermal Analysis. The glass transition temperature (T_g) was measured using differential scanning calorimeter (DSC Q2000, TA Instruments) with a heating rate of 10°C min^{-1} in a nitrogen environment. The thermal stability was observed by thermogravimetric analysis (TGA Q50, TA Instruments) with a heating rate of 10°C min^{-1} under nitrogen purge. The temperature of 5% weight loss was recorded as initial thermal degradation.

Scanning Electron Microscopy. Field emission scanning electron microscope (SEM, JEOL JSM-7401F) was used to study the morphology and distribution of the pigment particles. The surface morphologies of the samples were recorded with a Nanoscope III from Digital Instruments.

Atomic Force Microscopy (AFM). The atomic force microscope was operated in the tapping mode under ambient conditions using commercial silicon micro-cantilever probe tips (Veeco, RTESP5) with spring constants ranging between 20 and 80 N m^{-1} as specified by the manufacturer.

Coating Tests. Coating properties were evaluated according to ASTM methods including pencil hardness (D3363-05), impact resistance (G14), gloss rating (D523-89), MEK double rubs (D4752-06), cross-hatch adhesion (ASTM D3359-09e2), and pull-off adhesion (ASTM D 4541-85).

Electrochemical Impedance Spectroscopy (EIS). A cylindrical cell with the bottom area of 4.2 cm^2 was horizontally clamped to the rectangular coating sample (3″ × 6″) with the coating thickness of 6 mil. The cell body contains an O-ring to form a leak-proof seal. To simulate a weak acidic environment, 3.5% NaCl solution and 0.1 M HCl were used to adjust the pH value to 6. A Gamry Reference 600 System was used to perform the EIS measurements with a software control set up. A three electrode cell was used for the electrochemical characterization with a reference electrode (saturated Calomel), a counter electrode (niobium platinized mesh) and a working electrode as the coated sample. The impedance setup conditions with a frequency range from 50 kHz to 10 mHz with an amplitude of 10 mV (rms) at open circuit potential.

RESULTS

In this study, two types of polyesters were employed to evaluate the influence of pigmentation on the hybrid coatings. The first one was synthesized using 1,3- and 1,4-cyclohexanediacid (CHDA) (with a molar ratio of 1,3-/1,4-=1/2) and 2-butyl-2-ethyl-1,3-propanediol (BEPD). Previously reported by the Soucek group,[15] the oligoesters were developed for a high performance high-solid polyurethane coating. It was proven that the coatings showed good corrosion resistance, particularly thermal stability and UV-resistance because of its hydrophobicity, steric hindrance, and lack of aromatic rings.[9] Therefore, it was chosen as a baseline for comparison. However, in consideration of the high cost of the diacids (1,3-/1,4-CHDA) and diol, a more commercially viable polyester was polymerized using adipic acid (AA), isophthalic acid (IPA), 1,6-hexanediol (HD) and trimethylolpropane (TMP).[11] The 1,6-HD was selected to increase the flexibility, while TMP was used to increase the crosslink density as well as control the esterification rate. The oligoesters were characterized using IR, NMR, GPC, and acid number; and the spectral data (in Supporting Information data) was consistent with the previously reported data.[15] The oligoesters were formulated with HDI isocyanurate, alkoxysilane-modified isocyanurate, and TEOS oligomers as well as the pigment to form the polyurethane/polysiloxane hybrid coatings, as depicted in Scheme 1. The functionalized isocyanurate provided the covalent bonding between the organic phase and inorganic phase via a urea and a siloxane linkage.

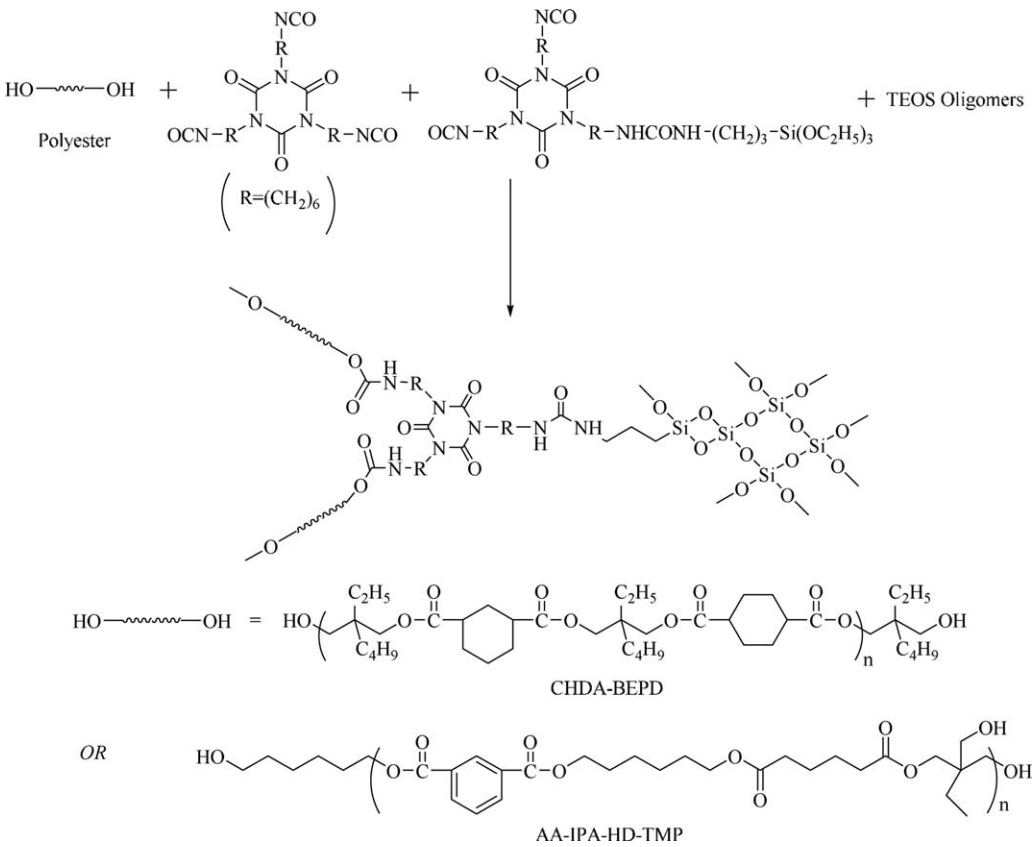

Scheme 1. The chemistry of the polyurethane/polysiloxane hybrid coatings.

Solid-State ^{29}Si NMR

The solid-state ^{29}Si NMR analysis was performed in order to investigate the formation of the Ti—O—Si bonds in the pigmented polyurethane/polysiloxane hybrid coatings. Figure 1(a–c) shows the NMR spectra obtained for the pigmented hybrid coating compositions based on CHDA-BEPD binder and for the control samples prepared without a polymer binder to aid resonance identification. Similar spectra were observed for the composition based on AA-IPA-HD-TMP binder. The control samples contained TEOS oligomer, TiO_2 and TEOS oligomer, APTMS serving as a coupling agent, TiO_2 and APTMS and TiO_2, APTMS and TEOS oligomer. The expanded $T^{0\text{-}3}$ region of the spectra [Figure 1(b)], shows that there are more than Si—O—Si bonds formed, and there are clear shifts in the spectra consistent with hetero Ti—O—Si bonds for the T^3. The TEOS and the polyurethane medium also appear to have an effect on the exact location of the resonances, as well as on the degree of condensation. The Q-region [Figure 1(c)], tells a similar story, but with the TEOS being more reactive toward the TiO_2 than the alkoxy silane under the reaction conditions used. The chemical shift at the Q^4 resonance showed predominately Si—O—Si whereas the others, Q^1, Q^2, and Q^3, exhibited shifts consistent with hetero Ti—O—Si bonding. The Q^3 shifted downfield from $\delta = -102.6$ ppm for TEOS oligomer to $\delta = -102.0$ ppm with incorporation of TiO_2 particles, and the Q^2 shifted from $\delta = -96.0$ ppm to $\delta = -92.5$ ppm. The degree of condensation changed depending on the sample and conditions. There is clearly less Q^2 when TiO_2 in the sample. The observed downfield shifts at the T and Q regions for the pigmented samples demonstrate of the formation of the hetero Ti—O—Si bonds for the analyzed compositions.

X-ray Photoelectron Spectroscopy (XPS) Analysis

To observe the interaction between the pigment particles and the hybrid binders, the pigmented polyurethane hybrid coating based on CHDA-BEPD and AA-IPA-HD-TMP polyesters with 40 wt % TiO_2 was analyzed by XPS. The surface of the sample was removed by $\sim$5 μm using microtome so as to probe the inside of the coating system. Figure 2 showed the XPS survey spectra of the pigmented hybrid coatings based on CHDA-BEPD and AA-IPA-HD-TMP polyesters, which contained carbon, oxygen, nitrogen, silicon, and titanium atoms. In both cases, the binding energies of all the elements appear at the same position as listed: C 1s (284.6 eV), O 1s (532.1 eV), N 1s (399.6 eV), Si 2s (152.6 eV), Si 2p (102.1 eV), and Ti 2p (458.1 eV). The nominal and theoretical chemical compositions of the two coating systems were summarized in Table III. The significant discrepancies in the concentration of titanium and carbon atoms between the nominal and theoretical compositions indicated that the titanium dioxide particles were embedded in the organic binder, which hide TiO_2 from exposure to the incident X-ray. As a result, the carbon concentration from the organic binder increased, whereas the titanium concentration dropped sharply.

To investigate the interaction between polysiloxane component and TiO_2 particles, the binding energy of the Si 2p peak was deconvoluted as depicted in Figure 3. In the hybrid polyurethane coating based on the CHDA-BEPD oligoester, the deconvolution

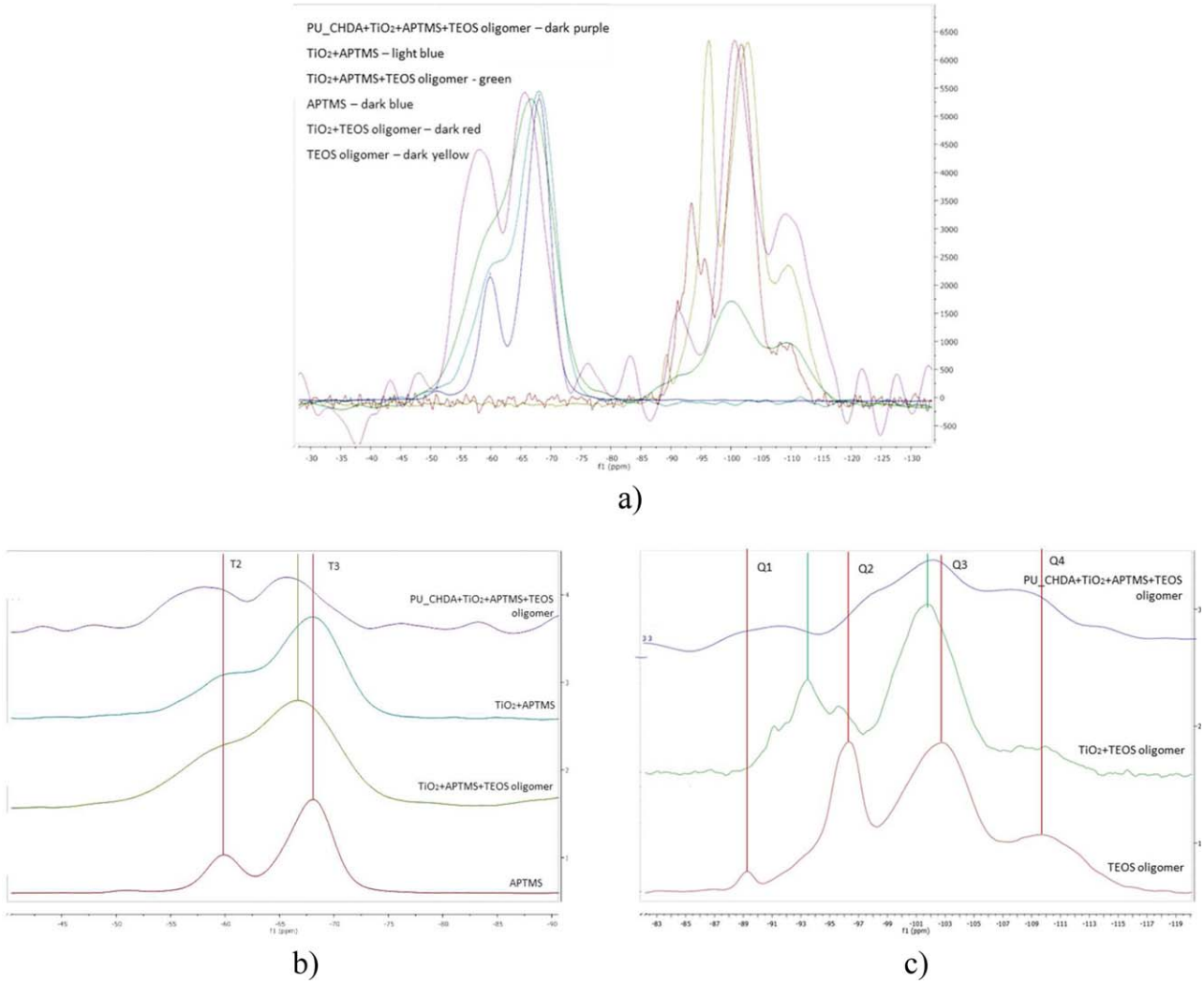

Figure 1. Solid-state ^{29}Si NMR spectra for pigmented polyurethane/polysiloxane hybrid coating compositions based on CHDA-BEPD and for the control samples for the whole spectral region (a) and expanded in the T-region, (b) and Q-region (c) (a) CHDA-BEPD (b) AA-IPA-HD-TMP. [Color figure can be viewed in the online issue, which is available at wileyonlinelibrary.com.]

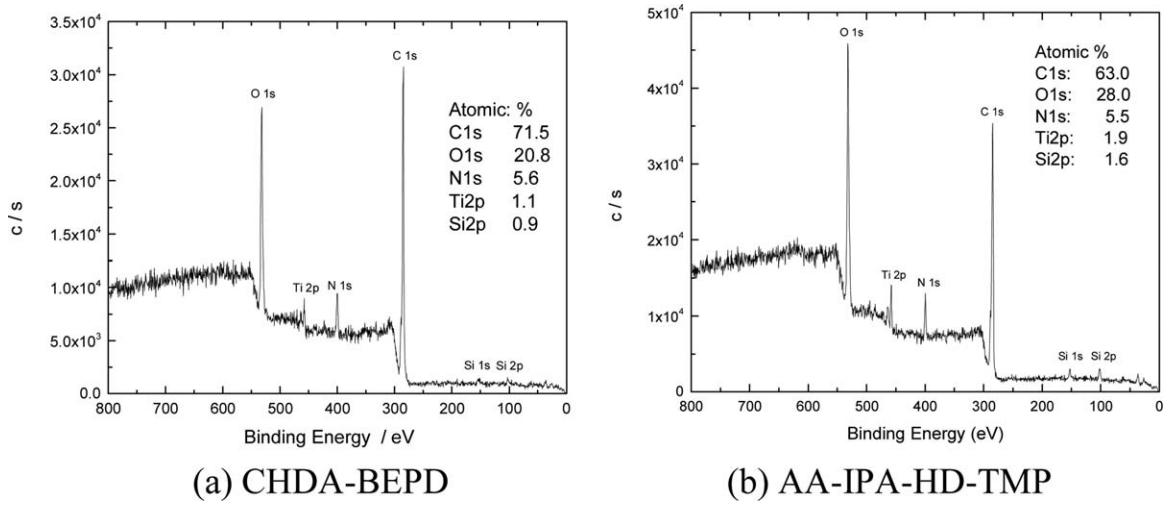

Figure 2. XPS survey spectra of pigmented polyurethane/polysiloxane hybrid coatings based on (a) CHDA-BEPD, (b) AA-IPA-HD-TMP (40 wt % TiO_2) (a) CHDA-BEPD (b) AA-IPA-HD-TMP.

Table III. Nominal and Theoretical atomic Composition at the Surface of the Pigmented Hybrid Coatings by Quantifying XPS Spectra

	CHDA-BEPD-based hybrid coating						AA-IPA-HD-TMP-based hybrid coating					
Elements	C	N	O	Ti	Si	H	C	N	O	Ti	Si	H
Nominal (%)	71.5	5.6	20.8	1.1	0.9	NI[a]	63.0	5.5	28.0	1.9	1.6	NI[a]
Theoretical (%)	36.1	3.8	28.8	24.0	1.9	5.3	34.1	3.8	31.6	24.0	1.9	4.6

[a] NI refers to "not identified."

of the Si 2p peak led to three single Gaussian curves centered at 101.69 eV, 102.67 eV, and 103.66 eV. The peaks at 101.69 eV and 102.67 eV were attributed to O—Si—O and O—Si—C, respectively.[31] The structure O—Si—O resulted from the condensation during the sol–gel process and the structure O—Si—C came from the coupling agent used in the formulation. The peak at 103.66 eV originated from the interaction between polysiloxane and the pigment particles.[32,33] Not surprisingly, similar findings were obtained for the AA-IPA-HD-TMP polyurethane hybrid coating. The deconvolution of the Si 2p peak yielded 101.35, 102.10, and 102.98 eV, which corresponded to O—Si—O, O—Si—C, and Ti—O—Si, respectively. Because of the lower electronegativity of Ti than Si, more charge transfer occurred from Ti to Si in the Ti—O—Si structure than in the Si—O—Si analog, which resulted in a higher binding energy of Si 2p in the Ti—O—Si structure. This result also corroborated the covalent bonding observed in the solid-state ^{29}Si NMR results.

Viscoelastic Properties

The viscoelastic properties of the pigmented hybrid coatings were investigated by dynamic mechanical thermal analysis (DMTA). Figure 4 showed the storage modulus (E') and tan δ of the pigmented coatings as a function of temperature. It was found that the glass transition temperature of the pigmented hybrid coatings decreased compared to the nonpigmented coatings as manifested from the storage modulus and tan δ curves. Moreover, for the pigmented coatings, increasing the amount of pigments improved the storage modulus below T_g, but did not have much influence above T_g. The pigmented polyurethane coatings based on AA-IPA-HD-TMP polyester showed higher storage modulus which was attributed to the rigidity of the phenyl ring in the backbone of the polymer binder. It was interesting that the variation of pigment concentration did not affect the glass transition temperature of the coatings as shown tan δ in (b) and (d). However, the peak intensity of tan δ reduced gradually as the pigment concentration increased from 10 to 40 wt %. The addition of the pigment particles into the hybrid coating apparently brought more anisotropy into the system. This was a consequence of the phase differences between the organic, inorganic sol–gel phase, and the inorganic pigments. The energy was easier to dissipate, which increased the damping properties and therefore the magnitude of tan δ.

Mechanical Properties

The tensile properties as a function of the pigment concentration in the coatings based on CHDA-BEPD and AA-IPA-HD-TMP oligoesters are shown in Figures 5 and 6, respectively. In general, the tensile modulus and tensile strength increased with increasing pigmentation, while the elongation-at-break reduced. The tensile strength of the pigmented polyurethane/polysiloxane hybrid coatings based on AA-IPA-HD-TMP polyester increased gradually from 8.50 to 13.65 MPa with the addition of TiO_2 from 0 (non-pigmented) to 40 wt %. The modulus showed the similar trend, increasing from 16.14 to 21.03 MPa as the amount of pigment increased. In contrast, the strain at break decreased slowly from 96 to 71% with increasing amount of TiO_2. In the CHDA-BEPD polyester based polyurethane hybrid coating system, a similar trend was found; the tensile strength

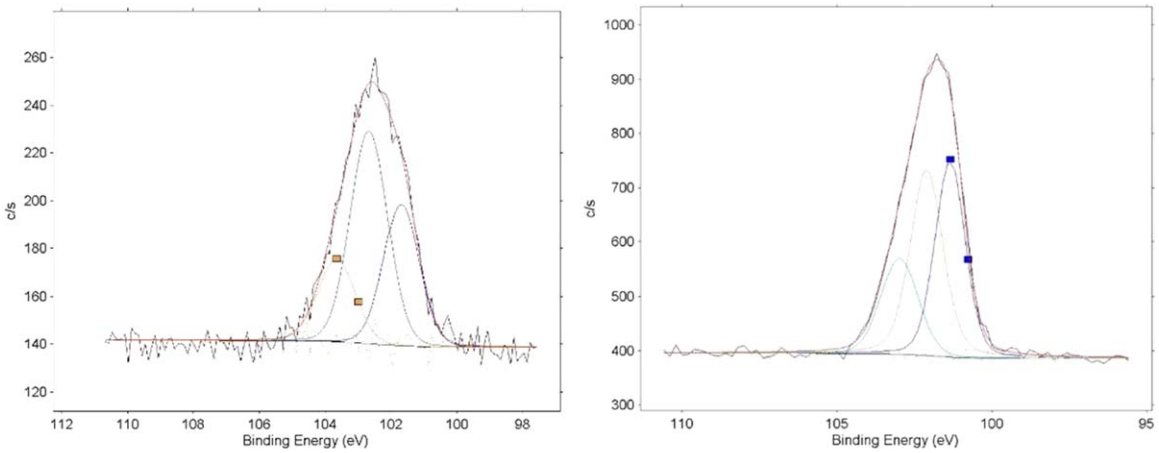

Figure 3. High resolution XPS spectra of Si 2p region with curve fitting; (a) CHDA-BEPD based; (b) AA-IPA-HD-TMP based. [Color figure can be viewed in the online issue, which is available at wileyonlinelibrary.com.]

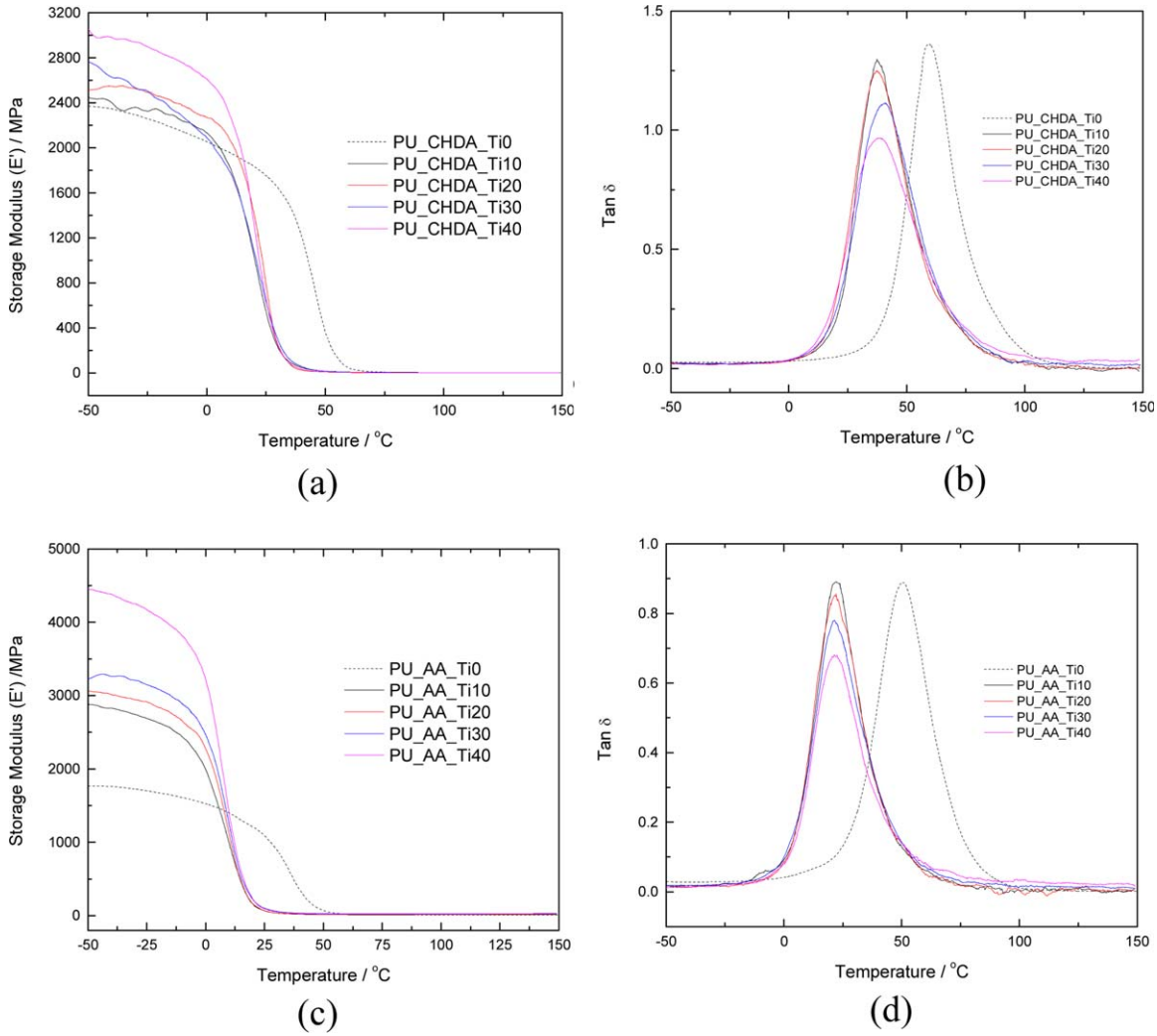

Figure 4. Influence of PVC on the storage modulus and tan δ value of the pigmented polyurethane hybrid coatings based on CHDA-BEPD (a,b) polyester and AA-IPA-HD-TMP (c,d) polyester. [Color figure can be viewed in the online issue, which is available at wileyonlinelibrary.com.]

increased from 4.24 to 7.18 MPa; the modulus increased from 8.88 to 10.05 MPa, while the strain at break reduced from 115 to 63%.

In the control polyurethane coating systems without TEOS and alkoxysilane, the modulus of the polyurethane based on AA-IPA-HD-TMP polyester increased from 12.75 to 22.79 MPa and

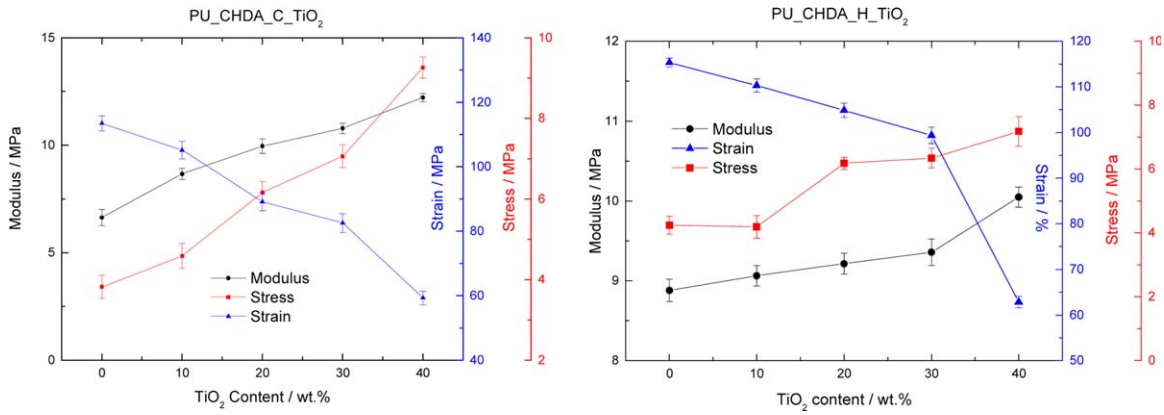

Figure 5. Modulus, stress, and strain versus TiO_2 content in pigmented polyurethane coatings based on CHDA-BEPD polyester: left: control; right: hybrid. [Color figure can be viewed in the online issue, which is available at wileyonlinelibrary.com.]

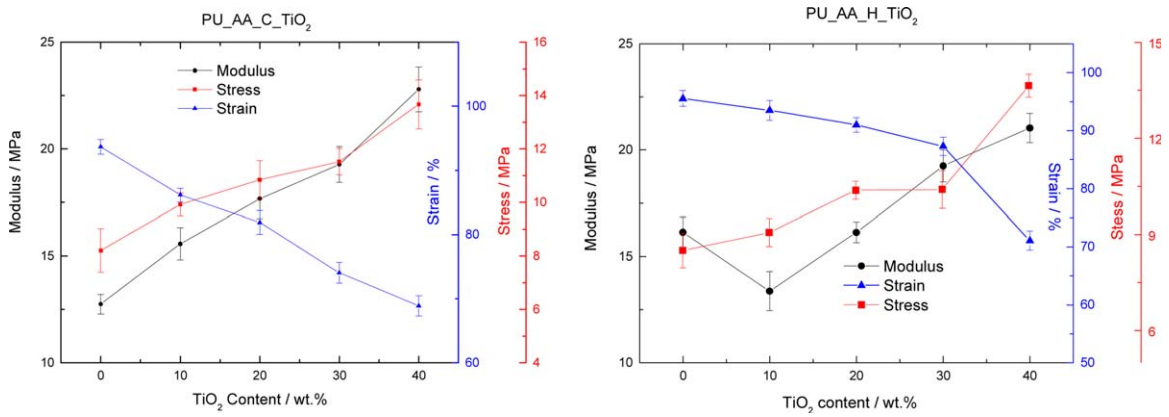

Figure 6. Modulus, stress, and strain versus TiO_2 content in pigmented polyurethane coatings based on AA-IPA-HD-TMP polyester: left: control; right: hybrid. [Color figure can be viewed in the online issue, which is available at wileyonlinelibrary.com.]

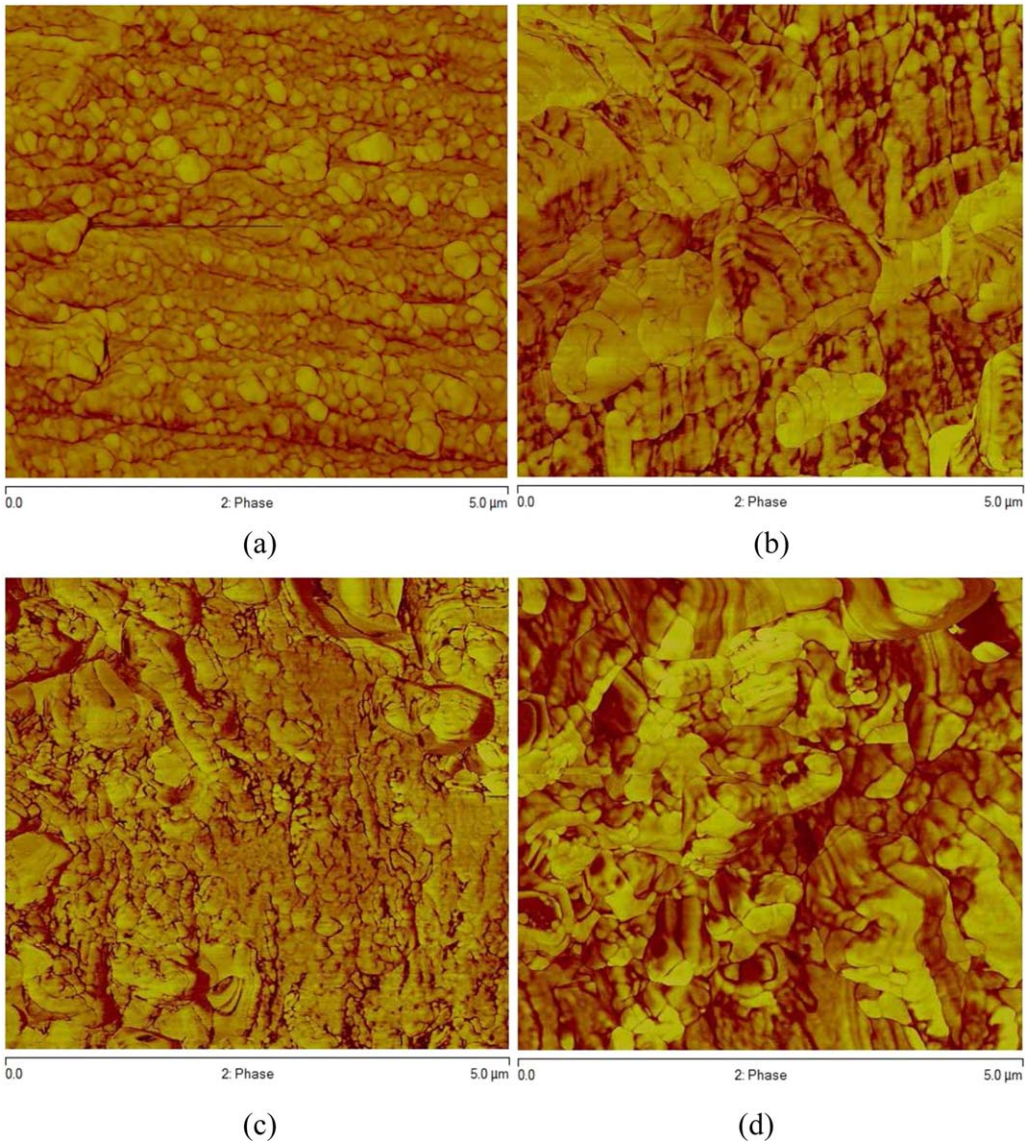

Figure 7. The AFM images of the TiO_2 pigmented polyurethane/polysiloxane hybrid coatings based on CHDA-BEPD polyester; (a) 10 wt %; (b) 20 wt %; (c) 30 wt %; (d) 40 wt %. [Color figure can be viewed in the online issue, which is available at wileyonlinelibrary.com.]

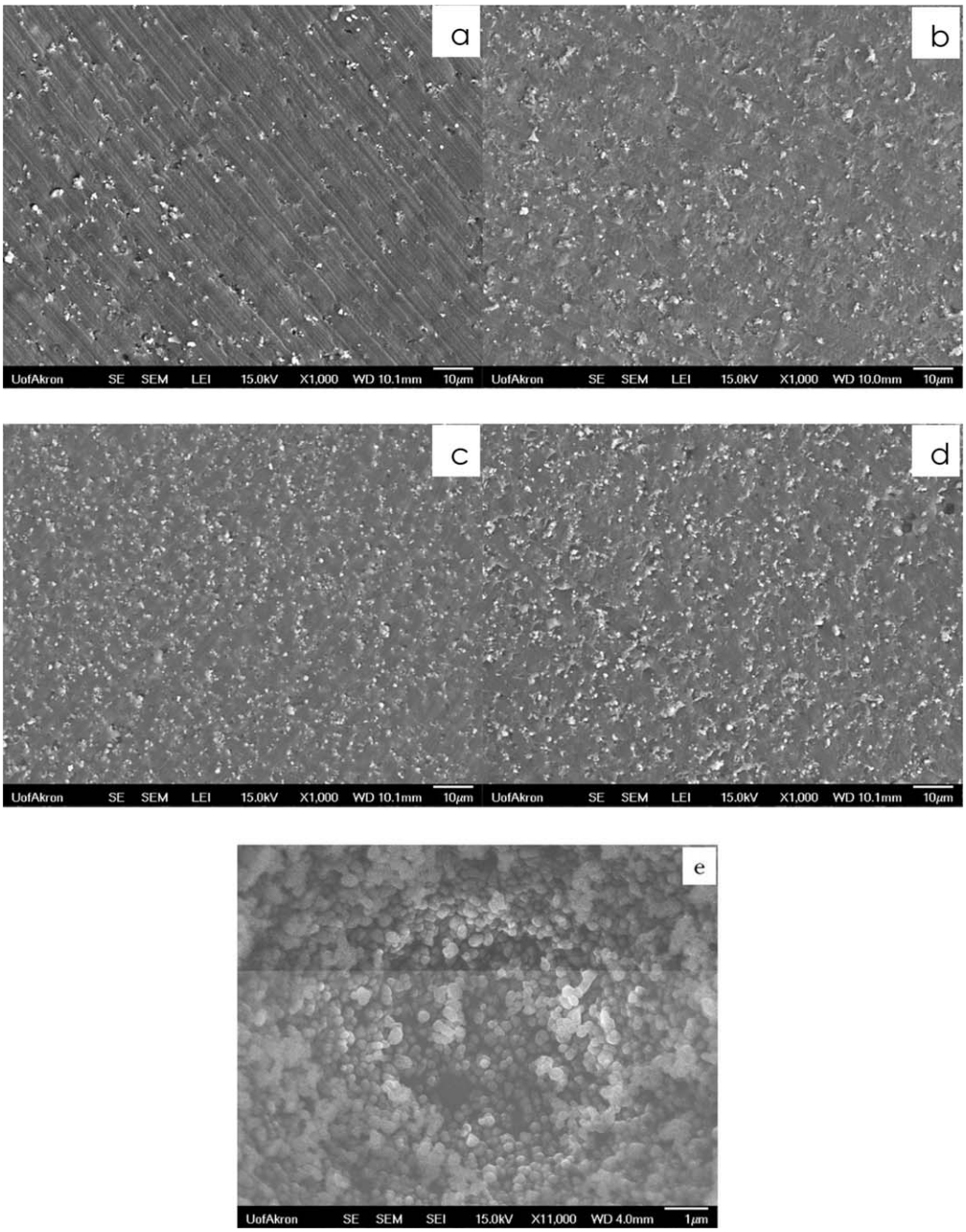

Figure 8. The SEM micrographs of the TiO_2 pigmented polyurethane coatings (control) based on CHDA-BEPD polyester; (a) 10 wt %; (b) 20 wt %; (c) 30 wt %; (d) 40 wt %; (e) TiO_2 particles.

the tensile strength shifted from 8.21 to 13.67 MPa when TiO_2 concentration increased from 0 to 40 wt %, while the elongation at break dropped from 94 to 69%. The coatings based on CHDA-BEPD polyester presented an increase in the modulus from 6.64 to 12.22 MPa as well as in the strength from 3.82 to 9.26 MPa with an increase in pigment concentration. The elongation was found to decrease from 113 to 59%.

The coatings based on AA-IPA-HD-TMP polyester showed higher tensile strength and modulus than the one based on CHDA-BEPD polyester both in nonpigmented and pigmented condition. CHDA and BEPD are bi-functional diacids and diols, respectively, which tend to form a linear polyester. In contrast, TMP has three hydroxyl groups which plays a role in forming crosslinked network. The crosslink density can be determined using eq. (1):

$$E' = 3\nu_e RT \quad (1)$$

where ν_e is the number of moles of elastically effective network chains per cubic meter of film and E' is the storage modulus. The crosslink density was calculated as 1042 and 465 mol m^{-3} for AA-IPA-HD-TMP polyester and CHDA-BEPD polyester, respectively. Therefore, it is not surprising that the AA-IPA-HD-TMP based coatings had better tensile properties.

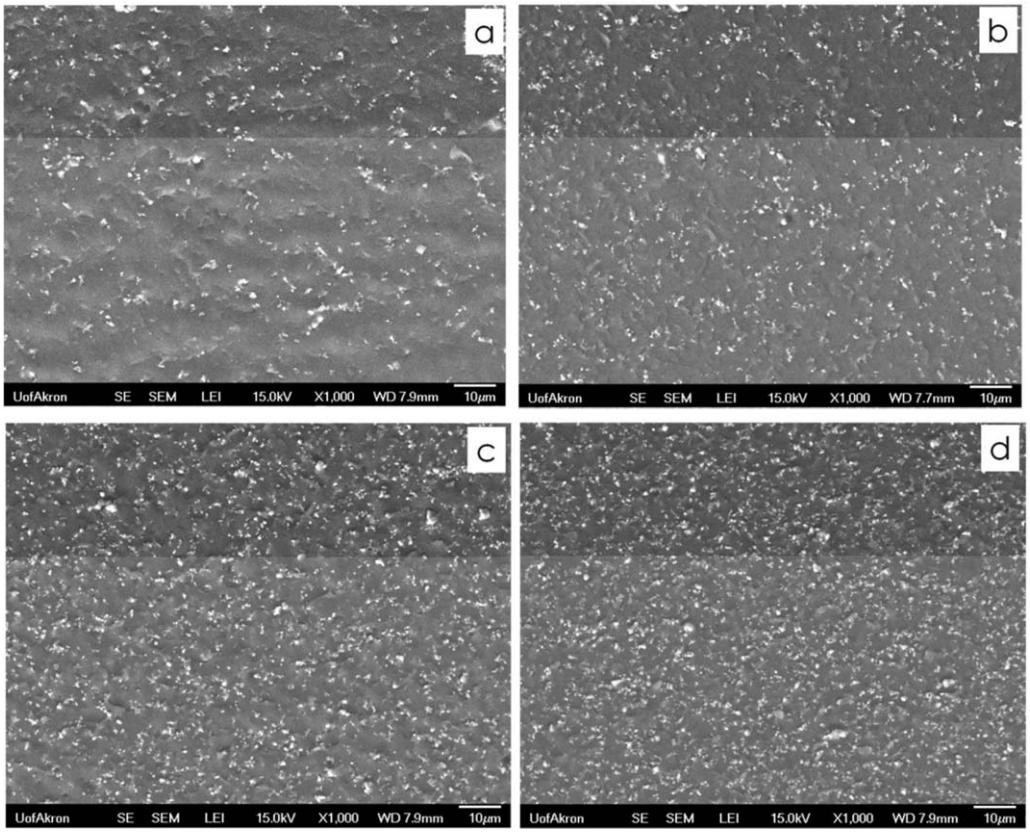

Figure 9. The SEM micrographs of the TiO_2 pigmented polyurethane/polysiloxane hybrid coatings based on CHDA-BEPD polyester; (a) 10 wt %; (b) 20 wt %; (c) 30 wt %; (d) 40 wt %.

Morphology

It is interesting and important to know that the distribution of the TiO_2 pigments in the polymeric binders since the microstructure of the coatings finally affect the coating performance and other properties. AFM and SEM were employed to investigate the pigment dispersion. After curing, the surface of the pigmented coatings was mainly composed of a thin layer of polymer binder. Therefore, all the coating films were microtomed by ~5 μm in order to remove the surface layer and probe the inner structure of the composite.

Figure 7 shows the tapping mode AFM phase images of the TiO_2 pigmented polyurethane/polysiloxane hybrid coatings based on CHDA-BEPD polyester with different concentration of pigmentation. It is well known that AFM obtains the phase images by determining the mechanical contrast of the hard and soft regions. In all the images, the darker regions resulted from the pigment particles. It was clear that the particles were dispersed uniformly without agglomeration with low loading of pigments, while the pigments tended to agglomerate when more pigments were introduced.

Figures 8(a–d) showed the SEM images of the control pigmented coating films with different TiO_2 loding level (10–40 wt %) and (e) revealed the raw TiO_2 particles as received. Figure 9 presented the SEM images of the pigmented hybrid coatings with incremental pigments. White represented the pigment particles, while the black background was the polymeric binder. Similar to what was observed in the AFM images, the pigment particles were distributed uniformly throughout the polymer binder both in the control and hybrid coatings. In Figure 8(e), the TiO_2 particles had a size distribution of 300–500 nm, while in all the pigmented coatings, the particle size had a wider distribution of 300–2000 nm, which meant that the particles distributed very well and uniformly.

Table IV. Glass Transition Temperature of the Pigmented Polyurethane Coatings based on CHDA-BEPD Polyester

Samples	T_g (°C)	Samples	T_g (°C)
PU_CHDA_C_Ti0	32	PU_CHDA_H_Ti0	32
PU_CHDA_C_Ti10	37	PU_CHDA_H_Ti10	32
PU_CHDA_C_Ti20	36	PU_CHDA_H_Ti20	31
PU_CHDA_C_Ti30	33	PU_CHDA_H_Ti30	27
PU_CHDA_C_Ti40	32	PU_CHDA_H_Ti40	28

Table V. Glass Transition Temperature of the Pigmented Polyurethane Coatings Based on AA-IPA-HD-TMP Polyester

Samples	T_g (°C)	Samples	T_g (°C)
PU_AA_C_Ti0	13	PU_AA_H_Ti0	20
PU_AA_C_Ti10	14	PU_AA_H_Ti10	10
PU_AA_C_Ti20	16	PU_AA_H_Ti20	11
PU_AA_C_Ti30	13	PU_AA_H_Ti30	12
PU_AA_C_Ti40	13	PU_AA_H_Ti40	11

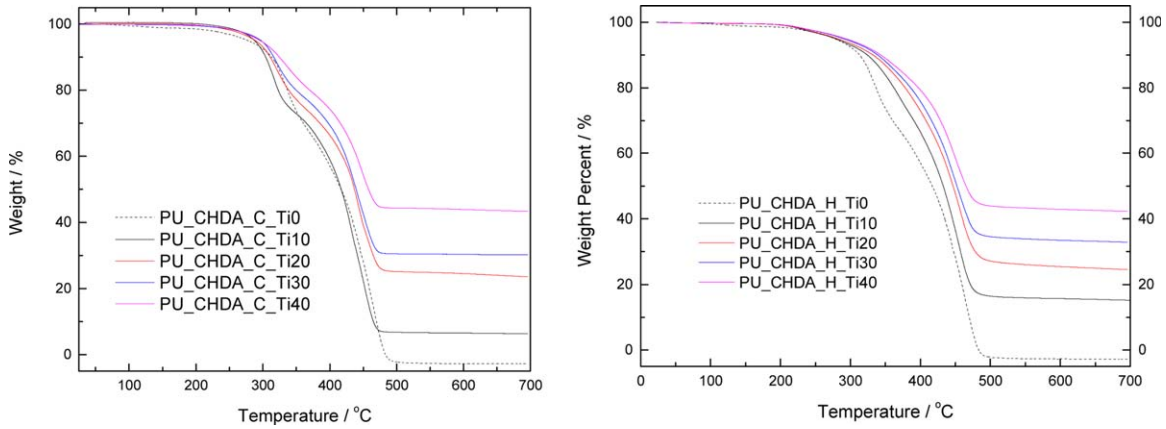

Figure 10. TGA Curves of pigmented polyurethane coatings based on CHDA-BEPD polyester (left: control; right: hybrid). [Color figure can be viewed in the online issue, which is available at wileyonlinelibrary.com.]

Thermal Analysis

The thermal behavior of the pigmented coatings were studied by differential scanning calorimetry (DSC) and thermal gravimetric analysis (TGA). Tables IV and V summarized the glass transition temperatures (T_g) of the pigmented coatings with various pigmentation volume concentration. Regarding the pigmented polyurethane coatings based on CHDA-BEPD polyester, the glass transition temperature dropped slightly from 32°C (nonpigmented) to 28°C (40 wt % pigmentation) for the hybrid coatings, while it increased from 32 to 37°C initially and then decreased to 32°C for the control samples. T_g of the ones based AA-IPA-HD-TMP polyester reduced from 20°C (nonpigmented) to 11°C (40 wt %), while it increased from 13 to 16°C (30 wt % pigment) in the beginning and dropped to 13°C again with 40 wt % pigmentation. It could be concluded that the addition of pigments did not affect the glass transition temperature in consideration of the slight variation.

Figures 10 and 11 showed the TGA thermograms of the pigmented polyurethance coatings based on CHDA-BEPD and AA-IPA-HD-TMP polyesters, respectively. The onset degradation temperatures at 5% weight loss were summarized in Tables VI and VII. In the hybrid coating systems, the degradation temperature of the pigmented coatings based on CHDA-BEPD polyester increased from 278°C (non-pigmented) to 294°C (40 wt % pigmentation) and that of the coatings based on AA-IPA-HD-TMP polyester raised from 305°C (nonpigmented) to 317°C (40 wt % pigmentation). Similar trend was found in the control coating systems without the inorganic sol–gel phase, the onset degradation temperature increased from 277 to 297°C for CHDA-BEPD based coatings and raised from 297 to 349°C for AA-IPA-HD-TMP based ones. The enhancement of the thermal stability was ascribed to the interaction between the polysiloxane phase and the pigment particles. It was also found that the onset degradation temperature of the hybrid coatings based on AA-IPA-HD-TMP polyester was higher than those based on CHDA-BEPD polyester. Looking at the chemical structure of the two types of polyurethanes, it is not surprising since the former one contained phenyl groups in the backbone, which was more heat resistant in comparison with the latter one. In addition, AA-IPA-HD-TMP polyester contained a trifunctional component, TMP, which provided a more highly crosslinked structure, and consequently improved the thermal stability.

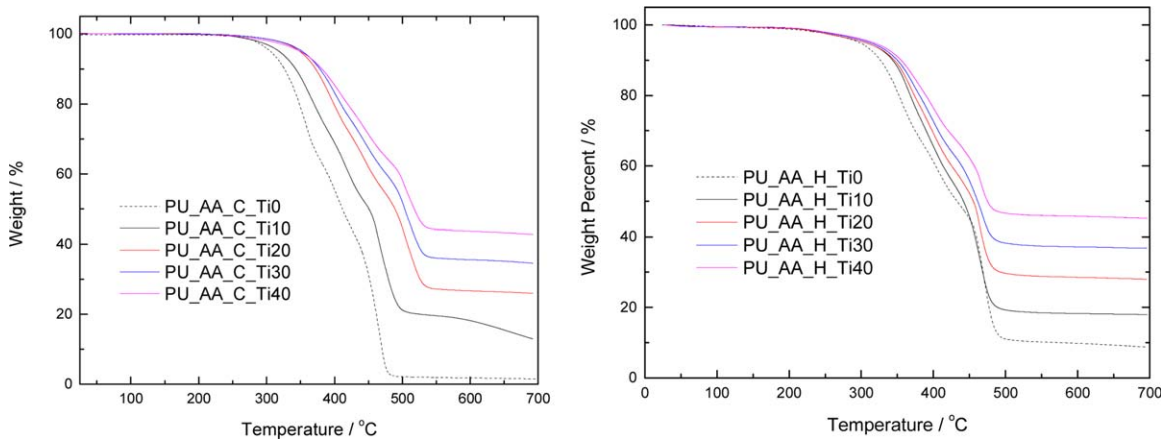

Figure 11. TGA thermograms of pigmented polyurethane coatings based on AA-IPA-HD-TMP polyester (left: control; right: hybrid). [Color figure can be viewed in the online issue, which is available at wileyonlinelibrary.com.]

Table VI. The Degradation Temperature at 5% Weight Loss of the Pigmented Polyurethane Coatings Based on CHDA-BEPD Polyester

Sample	T_d (°C)[a]	Sample	T_d (°C)[a]
PU_CHDA_C_Ti0	277	PU_CHDA_H_Ti0	278
PU_CHDA_C_Ti10	288	PU_CHDA_H_Ti10	279
PU_CHDA_C_Ti20	289	PU_CHDA_H_Ti20	282
PU_CHDA_C_Ti30	296	PU_CHDA_H_Ti30	291
PU_CHDA_C_Ti40	297	PU_CHDA_H_Ti40	294

[a] Degradation temperature at 5% weight loss.

Table VII. The Degradation Temperature at 5% Weight Loss of the Pigmented Polyurethane Coatings Based on AA-IPA-HD-TMP Polyester

Sample	T_d (°C)[a]	Sample	T_d (°C)[a]
PU_AA_C_Ti0	297	PU_AA_H_Ti0	305
PU_AA_C_Ti10	318	PU_AA_H_Ti10	305
PU_AA_C_Ti20	349	PU_AA_H_Ti20	306
PU_AA_C_Ti30	352	PU_AA_H_Ti30	312
PU_AA_C_Ti40	349	PU_AA_H_Ti40	317

[a] Degradation temperature at 5% weight loss.

General Coating Tests

The coating tests, namely, impact resistance, pencil hardness, solvent resistance, gloss, crosshatch adhesion, and pull-off adhesion, were performed on the pigmented coatings according to ASTM standards and the results are shown in Tables VIII (control) and IX (hybrid). All the coatings showed both excellent direct and reverse impact resistance, which were >100 kg cm^{-1}. The polyurethane hybrid coatings based on CHDA-BEPD and on AA-IPA-HD-TMP polyesters exhibited similar pencil hardness. Pigmentation enhanced the chemical resistance of the polyurethane hybrid coatings, but dramatically reduced the gloss at the incidence angle of both 20° and 60°. All the pigmented coatings showed better solvent resistance than the nonpigmented ones. The crosshatch adhesion of the coatings was not visibly affected by adding pigments, while the pull-off adhesion was slightly decreased. This phenomenon could be explained by the interaction between polysiloxane and the pigment particles, which resulted in less available spots for polysiloxane to interact with the substrate. The pigmented hybrid coatings presented higher pull-off adhesion (substrate/coating interfacial failure) over the control samples due to the existence of Si—O—Al bonding between the hybrid coatings and the metal substrate.

Electrochemical Impedance Spectroscopy (EIS)

The corrosion resistance of the pigmented coatings was evaluated by electrochemical impedance spectroscopy by immersing the coatings in a solution with a pH of 6. Figure 12 showed the Bode plots where the *y* axis was the impedance, which was an indication of the resistance of the coatings to the acidic environment. In general, all the curves showed capacitive behavior at high frequency and resistive behavior at low frequency. Figure 12(a) showed that the impedance increased after immersion for the clear coating (nonpigmented), which might be associated to the resistance the corrosion products gave to the system, but not related to the improvement of corrosion protection. Figure 12(b) presented the behavior of an intact coating that protected the system from water uptake and aggressive species like chlorides. Figure 12(c–e), illustrated the variation of the water uptake by the coatings as evidenced by the decrease in the impedance at low frequencies (<10 Hz) with increasing immersion time. At 10 wt % TiO_2, the corrosion resistance was improved. In addition, the pigmented hybrid coatings (except 40 wt %) showed impedance values above 10^{10} ohm-cm^2 at a low frequency of 0.01 Hz, 1–2 magnitudes higher than that of nonpigmented one (below 10^{10} ohm-cm^2). This observation suggested that the level of pigmentation loading had more effect on the corrosion resistance than the addition of sol–gel oligomers.

The water uptake after 211 days of immersion was quantified by the expression that Brasher and Kingbury developed as shown in eq. (2).[34] The results were summarized in Table X.

$$X = \frac{log\left(\frac{C_c}{C_{initial}}\right)}{log(80)} \quad (2)$$

where X_v is the volume fraction of water in the coating, C_c the coating capacitance at a specific time, and $C_{initial}$ the capacitance at the initial time of immersion. The dielectric constant of water

Table VIII. Coating Performance of the Pigmented Polyurethane Coatings (Control)

Sample	Direct impact resistance (kg cm^{-1})	Reverse impact resistance (kg cm^{-1})	Pencil hardness	MEK double rubs	Gloss 20°	Gloss 60°	Crosshatch adhesion	Pull-off adhesion (lb_f in^{-2})
PU_CHDA_C_Ti0	>100	>100	2H	161	139.6	198.2	5B	232 ± 5
PU_CHDA_C_Ti10	>100	>100	H	>200	69.7	87.4	5B	219 ± 2
PU_CHDA_C_Ti20	>100	>100	F	>200	61.8	83.3	5B	204 ± 3
PU_CHDA_C_Ti30	>100	>100	HB	>200	53.6	81.9	5B	197 ± 3
PU_CHDA_C_Ti40	>100	>100	F	>200	45.4	77.5	5B	187 ± 4
PU_AA_C_Ti0	>100	>100	F	>200	134.3	198.8	5B	217 ± 3
PU_AA_C_Ti10	>100	>100	HB	>200	64.7	86.4	5B	203 ± 5
PU_AA_C_Ti20	>100	>100	B	>200	52.2	80.9	5B	193 ± 4
PU_AA_C_Ti30	>100	>100	HB	>200	42.6	76.8	5B	185 ± 2
PU_AA_C_Ti40	>100	>100	B	>200	32.7	69.5	5B	177 ± 3

Table IX. Coating Performance of the Pigmented Polyurethane/Polysiloxane Hybrid Coatings

Sample	Direct impact resistance (kg cm^{-1})	Reverse impact resistance (kg cm^{-1})	Pencil hardness	MEK double rubs	Gloss		Crosshatch adhesion	Pull-off adhesion (lb_f in^{-2})
					20°	60°		
PU_CHDA_H_Ti0	>100	>100	H	142	132.6	189.8	5B	248 ± 8
PU_CHDA_H_Ti10	>100	>100	H	>200	72.5	85.8	5B	227 ± 5
PU_CHDA_H_Ti20	>100	>100	F	>200	62.6	82.3	5B	215 ± 4
PU_CHDA_H_Ti30	>100	>100	F	>200	56.9	82.7	5B	208 ± 2
PU_CHDA_H_Ti40	>100	>100	F	>200	47.5	79.6	5B	198 ± 3
PU_AA_H_Ti0	>100	>100	HB	143	136.3	190.7	5B	232 ± 4
PU_AA_H_Ti10	>100	>100	HB	>200	66.8	85.5	5B	221 ± 2
PU_AA_H_Ti20	>100	>100	HB	>200	51.3	81.1	5B	213 ± 3
PU_AA_H_Ti30	>100	>100	HB	>200	44.6	77.4	5B	201 ± 2
PU_AA_H_Ti40	>100	>100	HB	>200	29.7	71.2	5B	194 ± 5

was estimated to be 80. The capacitance values were calculated by fitting the impedance data with the equivalent circuit as shown in Figure 13.

More water was absorbed by the system as the TiO_2 content increased, and a detrimental effect was observed above 10 wt % TiO_2. An estimate of the surface area of the pigment particles with different PVC showed that 40 wt % pigmentation presented an area of 14.2 m^2, while 10 wt % gave a 3.55 m^2 surface area. This great difference in the surface area indicated that the pigment surface possibly would not be able to be covered by the hybrid binder with increasing PVC and thus led to more voids in the coating system, which explained the decreasing impedance with increasing PVC. The system without pigment experienced the lowest impedance values at a frequency of 0.01 Hz after 211 days, which was ascribed to a corrosion process taken place at the substrate surface. A difference of two orders of magnitude existed between the highest value of impedance (5.78×10^{10} ohm-cm^2) and the lowest (4.17×10^8 ohm-cm^2) which corresponded to 10 and 40 wt % pigmentation, respectively.

DISCUSSION

The polyurethane/polysiloxane hybrid materials have been studied for using as self-priming coatings in order to replace the chromate pretreatment. The addition of TEOS oligomer into the hybrid system was aiming at improving the adhesion between the coating and the metal substrate as well as inhibiting corrosion. The polysiloxane component, formed by the sol–gel process, has been proven to have a dramatic effect on the adhesion enhancement.[9,10,35–39] This is the first time that a study of film properties and corrosion resistance were reported for an inorganic/organic coating as a function of pigment loading.

Attempts (^{29}Si NMR and XPS) were made to establish evidence for pigment–sol–gel bonding. The XPS and NMR data strongly suggested the Si—O—Ti bonds[30,33] as depicted in Scheme 2. In the scheme, part of the TiO_2 particles are covalently bonded to the sol–gel precursors and some are free of chemical bonding. The hybrid binder refers to the polyurethane/polysiloxane hybrid coatings.

Because of the large surface area, the pigment particles tend to agglomerate if not treated correctly. The agglomerates normally act as the sites of stress concentration in the hybrid coating system and thus deteriorate the overall coating performance.[40] For the system in this study, the pigments are dispersed uniformly as shown by the SEM and AFM images. Before mixing into the polymer matrix, the particles had an average diameter of several hundred of nanometers. After formulated into the hybrid coatings, the particle size increased up to two microns, which had an agglomeration of three to four particles on average. Nevertheless, the agglomeration was so slight that it did not affect the overall coating performance as proved by other characterizations.

DMA studies showed decreasing glass transition temperature of the pigmented coatings when compared to the nonpigmented counterparts. Further addition of pigment concentration did not lead to additional reduction in T_g. This finding was in agreement with previous observations of the alumina/PMMA composites that the composites showed reductions of up to 25°C with as little as 0.5 wt % of alumina particles.[41] The authors argued that a large volume fraction of mobile polymer was generated through the addition inorganic components with a large surface area, which resulted in poor bonding of the polymeric components with the inorganic particles. For hybrid materials with pigments Roldugin *et al.*[42] proposed that the glass transition temperature of the polymer hybrid materials relied on two competitive factors: (1) the organic layer on the surface of the inorganic particles tended to increase the degree of freedom and the entropy of the system, which caused the decreasing glass transition temperature; and (2) the particles hindered the polymeric chains from coiling, thus decreased the entropy of disordering, which led to the increase of T_g. If the two factors counteract each other, there is no change in the glass transition temperature.

The tensile modulus and strength were increased by increasing the amount of pigment. This phenomena was attributed to the inter/intra molecular interaction between the polymer chains and between the polymer and the pigment particles, mainly the Si—O—Ti covalent bonding. The flexibility of the pigmented

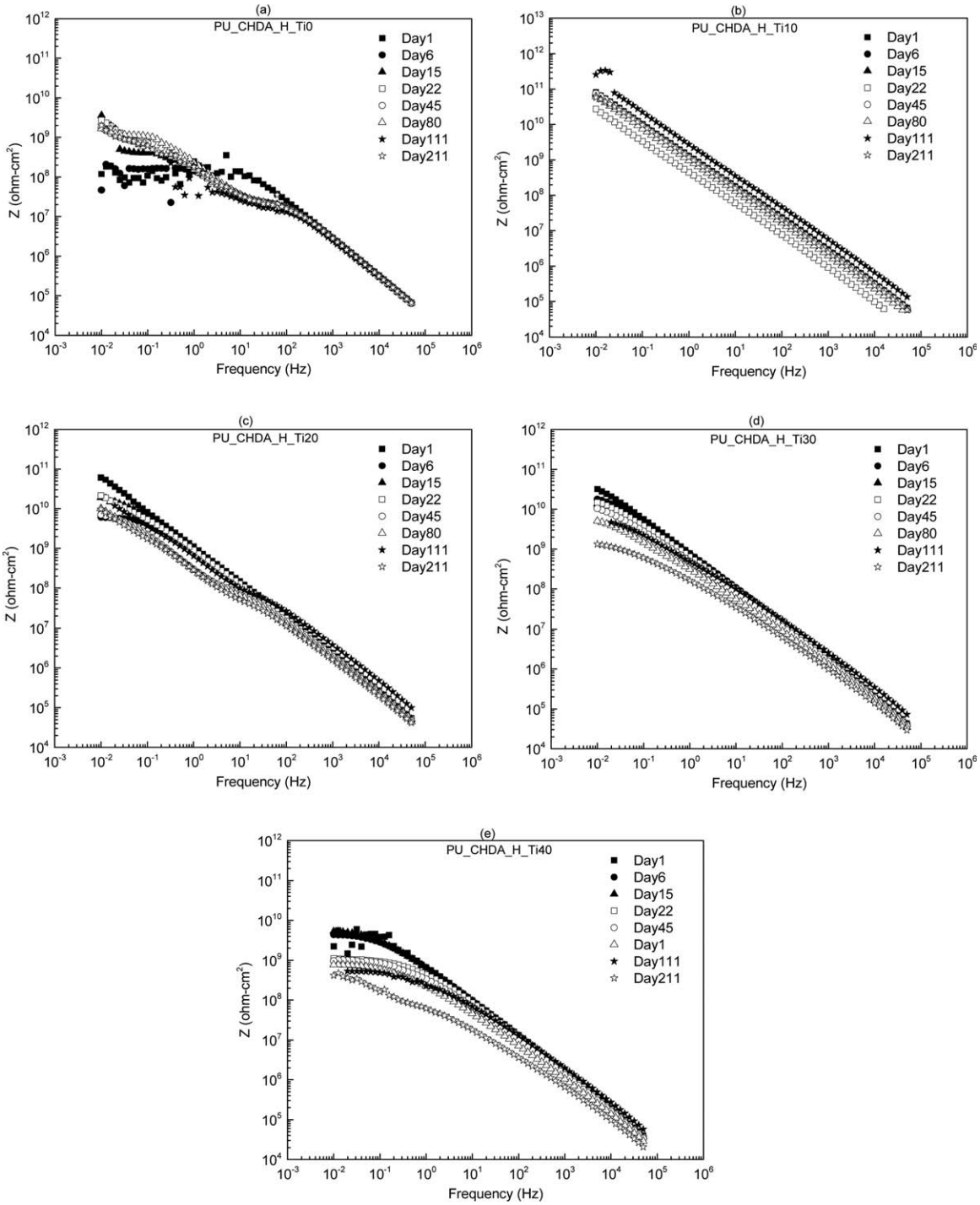

Figure 12. Bode plots of pigmented polyurethane/polysiloxane hybrid coatings with various PVC; (a) 0 wt %; (b) 10 wt % (c) 20 wt %; (d) 30 wt %; and (e) 40 wt %.

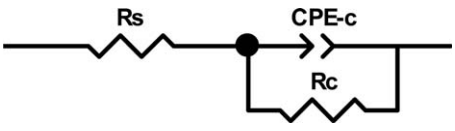

Figure 13. Equivalent circuit, where R_s is the electrolyte resistance, CPE-c is the constant phase element and associated to the coating capacitance, R_c is the coating resistance.

coating films was measured by the elongation-at-break. For both two pigmented coating systems, the elongation-at-break was reduced with increasing PVC. This trend was expected because the polymer chains were attached to the TiO_2 particles, which restricted the chain movement upon stretching. By comparing the tensile moduli, tensile strengths, and elongation-at-break of the hybrid coatings and the control ones, the absolute

Table X. Impedance and Water Content of the Pigmented Coatings after 211 Days of Immersion

TiO_2 concentration	Z, ohm-cm^2 (0.01 Hz)	Water content (%)
0	2.02×10^9	1.28
10	5.78×10^{10}	3.48
20	9.74×10^9	6.30
30	1.34×10^9	9.58
40	4.17×10^8	15.43

values were comparable, which implied that the pigmentation dominated the tensile properties.

The ultimate purpose of this study was to apply the pigmented coatings in protecting metals from corrosion, namely automotive and aircraft coatings. Therefore, the anticorrosion performance of these coatings are of great importance. As indicated by EIS studies, the nonpigmented hybrid coating showed the least impedance to the electrolyte as compared to the pigmented ones. Among the pigmented coatings, 10 wt % pigmentation excelled in providing the best corrosion protection properties. With the addition of pigment particles, it becomes more difficult for the electrolyte to penetrate through the micro-pores in the coating film.[43] In addition, the corrosive species require more time to reach the substrate since the diffusion path was elongated by introducing the pigment particles. However, more voids are formed at the organic/pigment interfaces when the amount of pigment is increased, which results in lowered impedance of the pigmented coatings. Because of the hydrophilic character of the TiO_2 particles, the water uptake of the pigmented coatings increase with increasing PVC, which consequently worsens the corrosion protection.

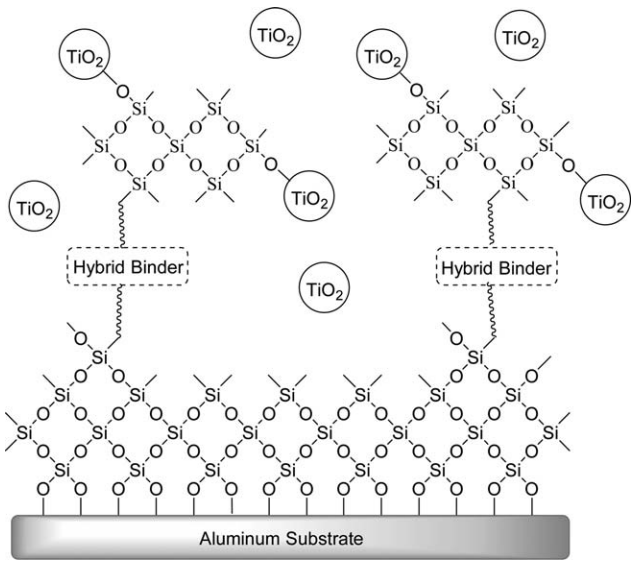

Scheme 2. The mechanism of the interaction between the hybrid binder and the pigment particles and the substrate.

CONCLUSION

The sol-gel precursors/oligomers reacted with the TiO_2 pigment to form Ti—O—Si bonding during the formation of the inorganic/organic hybrid films. The *in situ* sol–gel reactions did couple the particles enough to significantly affect the overall TiO_2 dispersion. Polyurethane/polysiloxane hybrid coatings were prepared with good pigment dispersion. The mechanical properties of the pigmented coatings were dominated more by the pigment loading than the addition of sol—gel precursors/oligomers. The thermal stability of the coatings was enhanced with increasing PVC while the pull-off adhesion was reduced by increasing the amount of TiO_2 pigment. The pigment loading did have an effect upon the corrosion resistance of the hybrid coatings. The coatings with 10 wt % pigmentation showed the best corrosion barrier properties as compared to the nonpigmented coating and the ones with higher PVC. As the pigment loading increased from 10 to 40 wt %, the corrosion resistance decreased.

ACKNOWLEDGMENTS

The authors acknowledge the support of the US Department of Defense Office of Corrosion Policy and Oversight and the research sponsor, the US Air Force Academy under agreement number FA7000-10-2-0013 and for FY11: W9132t-11-r-0043.

REFERENCES

1. Soucek, M. D. Hybrid Materials; Wiley-VCH Verlag GmbH & Co. KGaA, Weinheim, Germany, **2007**; p 433.
2. Wen, J. J.; Wilkes, K. G. L. *Mater. Res. Soc. Symp. Proc.* **1996**, *435*, 207.
3. Wright, M.; Uddin, A. *Solar Energy Mater. Solar Cells* **2012**, *107*, 87.
4. Fan, X.; Zhang, M.; Wang, X.; Yang, F.; Meng, X.; Fan, X.; Zhang, M.; Wang, X.; Yang, F.; Meng, X. *J. Mater. Chem. A* **2013**, *1*, 8694.
5. Wang, S.; Kang, Y.; Wang, L.; Zhang, H.; Wang, Y.; Wang, Y. *Sens. Actuat. B Chem.* **2013**, *182*, 467.
6. Wilkes, B. O. G. L.; Huang, H. *Polym. Prepr. Am. Chem. Soc. Div. Polym. Chem.* **1985**, *26*, 300.
7. Chattopadhyay, D. K.; Raju, K. V. S. N. *Prog. Polym. Sci.* **2007**, *32*, 352.
8. Soucek, M.; Ni, H. *J. Coat. Technol.* **2002**, *74*, 125.
9. Ni, H.; Johnson, A. H.; Soucek, M. D.; Grant, J. T.; Vreugdenhil, A. J. *Macromol. Mater. Eng.* **2002**, *287*, 470.
10. Ni, H.; Simonsick William, J.; Soucek Mark, D. New Developments in Coatings Technology; American Chemical Society, Washington, DC, **2007**; p 135.
11. Wicks, Z. W. Organic Coatings: Science and Technology, 3rd ed.; Wiley-Interscience, Hoboken, NJ, **2007**; p 23.
12. Chen, Y.; Lin, A.; Gan, F. *Appl. Surf. Sci.* **2006**, *252*, 8635.
13. Hwang, D. K.; Moon, J. H.; Shul, Y. G.; Jung, K. T.; Kim, D. H.; Lee, D. W. *J. Sol–Gel Sci. Technol.* **2003**, *26*, 783.

14. Mirabedini, S. M.; Mohseni, M.; PazokiFard, S.; Esfandeh, M. *Colloids Surf. A Physicochem. Eng. Aspects* **2008**, *317*, 80.
15. Rong, Y.; Chen, H. Z.; Li, H. Y.; Wang, M. *Colloids Surf. A Physicochem. Eng. Aspects* **2005**, *253*, 193.
16. Wetzel, B.; Rosso, P.; Haupert, F.; Friedrich, K. *Eng. Fract. Mech.* **2006**, *73*, 2375.
17. Yang, M.; Dan, Y. *Colloid. Polym. Sci.* **2005**, *284*, 243.
18. Yinghong, X.; Xin, W.; Xujie, Y.; Lude, L. *Mater. Chem. Phys.* **2003**, *77*, 609.
19. Zhu, M.; Xing, Q.; He, H.; Zhang, Y.; Chen, Y.; Pötschke, P.; Adler, H. J. *Macromol. Symp.* **2004**, *210*, 251.
20. Mirabedini, S. M.; Sabzi, M.; Zohuriaan-Mehr, J.; Atai, M.; Behzadnasab, M. *Appl. Surf. Sci.* **2011**, *257*, 4196.
21. Sabzi, M.; Mirabedini, S. M.; Zohuriaan-Mehr, J.; Atai, M. *Prog. Org. Coat.* **2009**, *65*, 222.
22. Chen, J.; Zhou, Y.; Nan, Q.; Sun, Y.; Ye, X.; Wang, Z. *Appl. Surf. Sci.* **2007**, *253*, 9154.
23. Chen, L.; Shen, H.; Lu, Z.; Feng, C.; Chen, S.; Wang, Y. *Colloid. Polym. Sci.* **2007**, *285*, 1515.
24. Gamble, L.; Hugenschmidt, M. B.; Campbell, C. T.; Jurgens, T. A.; Rogers, J. W. *J. Am. Chem. Soc.* **1993**, *115*, 12096.
25. Gamble, L.; Jung, L. S.; Campbell, C. T. *Langmuir* **1995**, *11*, 4505.
26. Iguchi, N.; Cady, C.; Snoeberger, R. C., III; Hunter, B. M.; Sproviero, E. M.; Schmuttenmaer, C. A.; Crabtree, R. H.; Brudvig, G. W.; Batista, V. S. Characterization of Siloxane Adsorbates Covalently Attached to TiO2, Physical Chemistry of Interfaces and Nanomaterials, **2008**; *7034*, 340.
27. Dworak, D. P.; Soucek, M. D. *Macromol. Chem. Phys.* **2006**, *207*, 1220.
28. Hoebbel, D.; Nacken, M.; Schmidt, H.; Huch, V.; Veith, M. *J. Mater. Chem.* **1998**, *8*, 171.
29. Ni, H.; Daum, J. L.; Thiltgen, P. R.; Soucek, M. D.; Simonsick, W. J., Jr., Zhong, W.; Skaja, A. D. *Prog. Org. Coat.* **2002**, *45*, 49.
30. Ni, H.; Aaserud, D. J.; Simonsick, W. J., Jr.; Soucek, M. D. *Polymer* **2000**, *41*, 57.
31. Abad, J.; Gonzalez, C.; de Andres, P. L.; Roman, E. *Phys. Rev. B* **2010**, *82*, 165420.
32. Molina, C.; Dahmouche, K.; Hammer, P.; Bermudez, V. D. Z.; Carlos, L. D.; Ferrari, M.; Montagna, M.; Gonçalves, R. R.; Oliveira, L. F. C.; Edwards, H. G. M.; Messaddeq, Y.; Ribeiro, S. J. L. *J. Braz. Chem. Soc.* **2006**, *17*, 443.
33. Zhu, L. Q.; Zhang, L. D.; Fang, Q. *Appl. Phys. Lett.* **2007**, *91*, 3.
34. Brasher, D. M.; Kingsbury, A. H. *J. Appl. Chem.* **1954**, *4*, 62.
35. Ni, H.; Simonsick, W. J.; Skaja, A. D.; Williams, J. P.; Soucek, M. D. *Prog. Org. Coat.* **2000**, *38*, 97.
36. Ni, H.; Skaja, A. D.; Sailer, R. A.; Soucek, M. D. *Polym. Prepr. Am. Chem. Soc. Div. Polym. Chem.* **1998**, *1*, 367.
37. Ni, H.; Skaja, A. D.; Sailer, R. A.; Soucek, M. D. *Macromol. Chem. Phys.* **2000**, *201*, 722.
38. Ni, H.; Skaja, A. D.; Soucek, M. D. *Prog. Org. Coat.* **2000**, *40*, 175.
39. Ni, H.; Skaja, A. D.; Soucek, M.; Simonsick, D. J. W. J.; Zhong, W. *Polym. Mater. Sci. Eng.* **1999**, *40*, 6.
40. García, M.; Marchese, G. J.; Ochoa, N. A. *J. Appl. Polym. Sci.* **2010**, *118*, 2417.
41. 41. Ash, B. J.; Siegel, R. W.; Schadler, L. S. *J. Polym. Sci. B Polym. Phys.* **2004**, *42*, 4371.
42. Roldugin, V. I.; Serenko, O. A.; Getmanova, E. V.; Karmishina, N. A.; Chvalun, S. N.; Muzafarov, A. M. Doklady Physical Chemistry; Springer, **2013**; p 449.
43. Kalendová, A. *Prog. Org. Coat.* **2003**, *46*, 324.